Decision Analytics Journal 12 (2024) 100512

Contents lists available at ScienceDirect

Decision Analytics Journal

journal homepage: www.elsevier.com/locate/dajour

A generalization of the Topological Tail Dependence theory: From indices to individual stocks

Hugo Gobato Souto [a], Amir Moradi [b,*]

[a] Institute of Mathematics and Computer Sciences at University of São Paulo, Av. Trab. São Carlense 400, 13566-590 São Carlos (SP), Brazil
[b] HAN University of Applied Sciences, Ruitenberglaan 31, 6826 CC Arnhem, The Netherlands

ARTICLE INFO

Keywords:
Topological Tail Dependence
Financial econometrics
Persistent homology
Stock realized volatility
Wasserstein Distance

ABSTRACT

This study investigates the Topological Tail Dependence (TTD) theory's applicability to individual stock volatility and high dimensions. Utilizing a comprehensive dataset from the S&P 100, the research employs various methodologies to test the predictions and implications of the TTD theory. The theory's main prediction of Wasserstein Distance's predictive utility, particularly in nonlinear models during volatile periods, is confirmed. The research suggests extending the TTD theory's application to various financial instruments and incorporating dynamic topological features to enhance understanding market dynamics. This study validates the TTD theory for individual stocks and highlights the necessity of topological considerations in financial modeling, promising advancements in financial econometrics and risk management strategies.

1. Introduction

The intricate dynamics of financial markets and their susceptibility to external shocks have perennially captivated the interest of researchers and practitioners alike [1–3]. For instance, Cetorelli and Gambera [4] explores the how the structure of the banking financial markets plays a crucial role in shaping the dynamics of capital accumulation and economic growth, while [5,6] and [7] studies the phenomenon of volatility spillovers between financial markets, especially in the context of globalized economies. The insights provided by these studies are directly relevant to understanding and exploiting the nature of current global financial markets, where this paper also contributes to.

Within this realm, the forecasting of stock realized volatility remains a cornerstone of financial econometrics, portfolio management, and risk assessment [8–10]. For example, Atkins et al. [11] demonstrates that news-derived information significantly improves the prediction of volatility movements over price movements, highlighting the importance of qualitative factors in volatility forecasting. Similarly, Bonato et al. [12] shows that realized skewness and kurtosis enhance the prediction of realized volatility across multiple time horizons, underscoring the value of incorporating higher moments of return distributions in forecasting models.

Moreover, Bašta and Molnár [13] explores the comovement of volatility between the equity and oil markets, finding that such relationships are time-scale dependent, which further complicates volatility forecasting but also opens up new avenues for more nuanced models. Expanding on these themes, Liu et al. [14] introduces an innovative approach by decomposing trading volume to improve volatility forecasts, thereby providing a fresh perspective on the volume-volatility relationship. In the context of advanced forecasting techniques, Tang et al. [15] employs optimized deep learning models to predict Bitcoin volatility, achieving significant improvements in accuracy, while Zhang et al. [16] highlights the superiority of neural networks over traditional models in forecasting intraday realized volatility by capturing complex latent interactions.

Incidentally, in the last years, the amount of attention paid to machine learning models for forecasting stock realized volatility in the scientific literature has considerably increased [17–19]. To give a few examples, Souto [17] evaluates the TimesNet model for forecasting realized volatility and shows that it is not superior to existing benchmark models, highlighting the ongoing need for model enhancements in volatility forecasting, while [20] introduces a novel Convolutional Neural Network (CNN)-Long Short Term Memory (LSTM) hybrid model specifically designed for predicting gold volatility, achieving substantial improvements over benchmark models in this task. This work underscores the effectiveness of hybrid architectures in capturing both static and dynamic characteristics of time series data, similar to how [21] combines Feedforward Neural Networks with LightGBM to improve the accuracy and robustness of volatility predictions. Both studies illustrate the power of combining different machine learning techniques to tackle the complex and nonlinear nature of financial data.

Finally, Bucci [22] and Lei et al. [23] both emphasize the superiority of deep learning models like LSTM and Temporal Convolutional Networks (TCN) over traditional econometric methods.

* Corresponding author.
E-mail addresses: hgsouto@usp.br (H.G. Souto), amir.moradi@han.nl (A. Moradi).

https://doi.org/10.1016/j.dajour.2024.100512
Received 8 March 2024; Received in revised form 19 August 2024; Accepted 20 August 2024
Available online 26 August 2024

These and other studies collectively represent the many developments in both theory and practice have been done in the realized volatility literature, though among all these developments, the use of Persistent Homology (PH) theory and derived techniques is presumably one of the most extraordinary and interesting, with its successful application ranging from corporate and systemic financial stability [24–27] to investment strategies [28,29] and stock realized volatility forecasting [30,31]. Nonetheless, it was not until the work of Souto [30] that the literature had a proposed theory to explain the success of the use of PH in portfolio and risk management. He introduces the Topological Tail Dependence (TTD) theory to explain this success by connecting the mathematical theory behind PH and the finance tail dependence theory [32,33].

This paper expands the work of Souto [30] by testing the TTD theory not only using stock indices. Although the assumption that findings applicable to stock indices can be seamlessly extrapolated to individual stocks often holds true, at times it can overlook the nuanced and often divergent behaviors between these two entities, influenced by idiosyncratic factors, sectoral dynamics, and investor sentiment [34]. This distinction underscores the necessity of validating the TTD theory's efficacy at the individual stock level, ensuring that its predictive capabilities are not confined to the aggregated market movements reflected in indices. Moreover, though [30] affirms that the TTD theory could be seen as a generalization of the finance tail dependence theory for high dimensions, his paper only uses six dimensions (stock indices) when putting the TTD theory to the test. As a result, by exploring a great number of individual stocks, one could also test whether the TTD theory indeed works for high dimensions (e.g., above 20 stocks).

Consequently, given the current gap in the finance literature of testing the TTD theory with individual stocks and in high dimensions, this study aims to close this gap and contribute to the theoretical development of the realized volatility literature. Adopting a rigorous empirical approach, this study employs a comprehensive dataset comprising realized volatility measures of 80 individual stocks present in the S&P 100, meticulously selected to ensure continuity and representativeness. The empirical investigation unfolds through a three-pronged methodology: a linear regression analysis, a Granger causality framework adapted for both linear and nonlinear models, and an innovative application of Shapley Additive Explanations (SHAP) values within a machine learning context to test one of the main implications of the TTD theory.

This research endeavors to make two scientific contributions to the realized volatility literature. Firstly, by testing and extending the TTD theory to individual stocks and in high dimensions, allowing researchers and practitioners to use the TTD theory to enhance their decision making regarding portfolio and risk management. Secondly, this research gives more evidence for the TTD theory, proving further indication that an exploration and even extension of this theory can likely yield promising results for researchers regarding the understanding of the stock market and for practitioners concerning the use of topological information for better decision making in the context of portfolio and risk management. On the other hand, the potential skepticism regarding the novelty of this research is addressed by emphasizing the critical need for theory validation across different financial securities. The generalization of the TTD theory to individual stocks and high dimensions not only tests the theory's veracity and robustness but also expands its applicability, thereby enhancing its utility for a broader spectrum. Such validation exercises are indispensable in the iterative process of theory refinement and development in scientific inquiry [35–40]. Last but not least, although this paper and [30] both explore the TTD theory, this paper distincts itself by testing TTD for individual stocks and in high dimensions and utilizing a more robust testing methodology, which exploits a robust linear regression analysis method, a modified Granger causality framework, and SHAP values.

Finally, the remainder of this paper is structured as follows: Section 2 presents a brief description of the TTD theory and important concepts for its understanding, such as PH and Wasserstein Distance (WD). Section 3, on the other hand, thoroughly explain the methodology used in this study to put the TTD theory to the test in the context of individual stocks and high dimensions. While Section 4 presents and discusses the results of the empirical tests performed to test the TTD theory, Section 6 concludes the paper by summarizing the key findings of this research and their implications, and by proposing future research avenues that researchers can follow based on the results of this study.

2. Topological tail dependence theory

Before going into the TTD theory, concepts such as Betti numbers, PH and WD should be understood. Hence, if the reader is not familiar with these concepts from Topology theory, please see [41] and [30]. However, a brief revision of these concepts can be found below:

PH is a methodological process for uncovering the topological characteristics of data. This process involves: (1) plotting the data points, (2) enveloping these points with disks or spheres of diameter ϵ, and establishing connections between points when their respective spheres intersect, (3) estimating the quantity of d-dimensional holes using Betti numbers, (4) iterating this procedure for a range of ϵ values, and finally (5) constructing a PH diagram that chronicles the emergence and resolution of each Betti number across dimensions for varying ϵ values. This process can also be visualized in Figs. 1, 2, and 3, which is an example based on the lecture of Rieck [42].

Subsequently, the topological attributes of two datasets or time frames can be compared by evaluating their respective PH diagrams using the WD metric in order to model the topological change in time or dataset.

Now considering the TTD theory, only a brief explanation of this theory is presented in this paper to ensure sparsity. If the reader is interested in the details behind this theory, please see [30].

The TTD theory exploits the phenomenon suggested by the Financial Tail Dependence Theory [33,43,44] that there is an increase in absolute stock correlations during financial downturns and also preceding such downturns as discovered by Jebran et al. [45]. In other words, not only do the absolute stock correlations increase in magnitude during financially stressful times as the Financial Tail Dependence Theory predicts, but also preceding such periods, albeit to a less extent. A real life example of the COVID financial crisis can be found in Figs. 4, 5, and 6 when considering the stock indexes Standard and Poor's 500 (S&P 500), Dow Jones Industrial Average (DJIA), and Russell 2000 Index (RUT).

Hence, the variation in absolute stock correlations between two distinct periods could serve as a predictive marker for impending financial turbulence by establishing a threshold during regular periods. However, this method's efficacy is limited by the 'curse of dimensionality' (thus, not being useful for portfolio management of portfolios with a great number of stocks) and fails to discern nonlinear and intricate relationships within the data [46,47]. Such limitations are circumvented through the adoption of PH techniques, utilizing WD or L^n norms of Persistent Landscapes (which remain unaffected by such challenges [46,47]) to properly model the phenomenon found by Jebran et al. [45] and use this information for better decision making and forecasting tasks. This explains for the success of the adoption of PH methods in recent studies to foresee financial volatile periods [24–27] and better perform portfolio management [28,29] and realized volatility forecasting [30,31].

As a result of this theory, we can anticipate a positive relationship between lagged WD and realized volatility. This is the case since prior to and during financial downturns, equities exhibit a fast increase in their joint correlation, and this increase in joint correlation can be effectively captured through the use of WD as a measure of market structure change, even in high dimensions where other methods fail due to the aforementioned curse of dimensionality. Since WD captures the extent of structural changes in the market, including increased stock

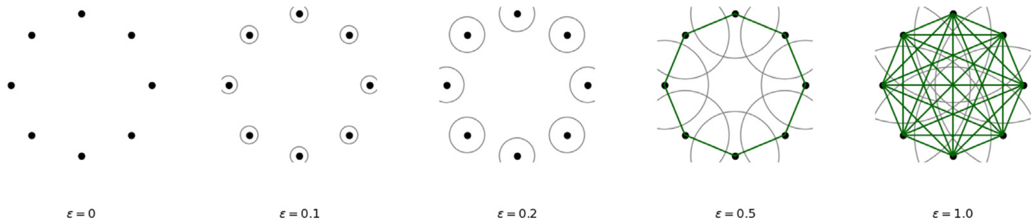

Fig. 1. Data points enveloped by spheres of different diameters (inspired by Rieck [42]).

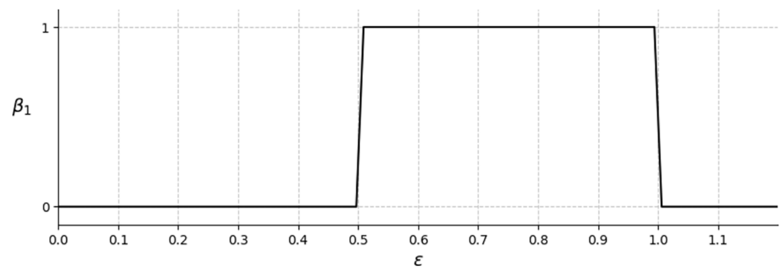

Fig. 2. 1st Betti number for each ϵ (inspired by Rieck [42]).

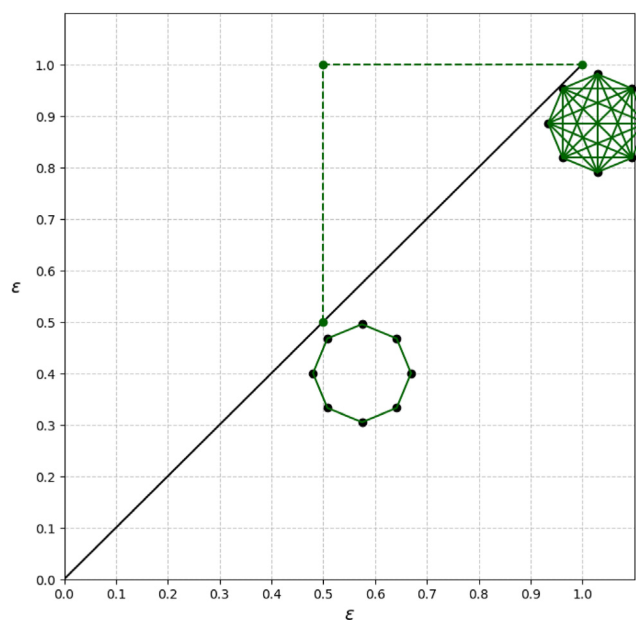

Fig. 3. Persistence homology graph for β_1 (inspired by Rieck [42]).

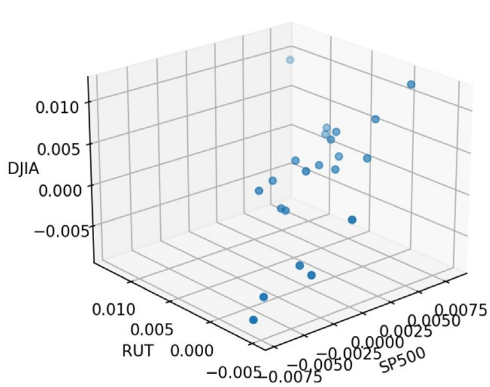

Fig. 4. 3D scatter plot from 16 December 2019 until 16 January 2020 (Normal Period) [30,31].

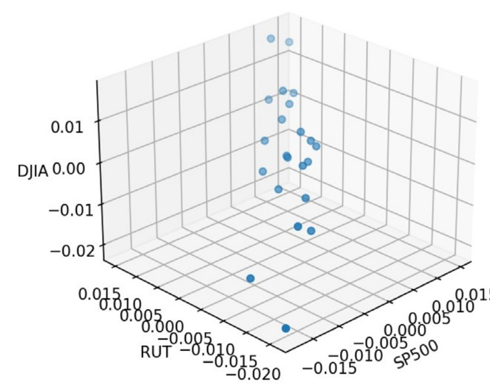

Fig. 5. 3D scatter plot from 17 January 2020 until 19 February 2020 (Preceding Period) [30,31].

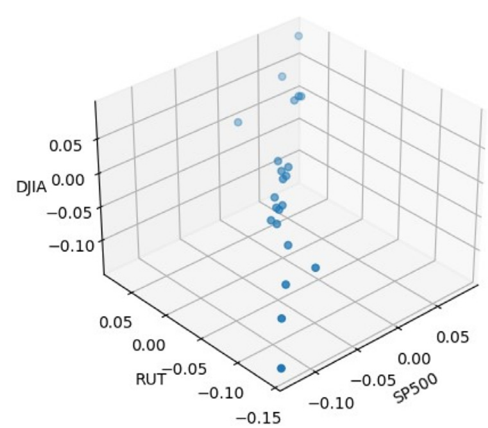

Fig. 6. 3D scatter plot from 20 February 2020 until 23 March 2020 (Turbulent Period) [30,31].

correlations and clustering during high volatility periods, its lagged, and especially top percentile, values correlates positively with realized volatility. As market structures become more interdependent prior to turbulent periods, the WD becomes more pronounced, indicating that higher realized volatility values are likely to occur on the upcoming days. It is worth mentioning that while there is a fast increase in the interdependence of stock prior to turbulent periods, the converse is not true from turbulent periods to normal periods as the transition is smoother and takes longer.

3. Research design

3.1. Sample

This study employs a comprehensive dataset comprising daily realized volatility (RV) measures from individual stocks to rigorously examine the applicability of the TTD theory beyond the realm of stock indices. Specifically, the dataset encompasses daily realized volatility data for a total of 80 constituents stocks from the S&P 100 index that have maintained continuous trading activity during the period from July 1, 2007, to June 30, 2021. This timeframe was deliberately chosen to encapsulate a broad spectrum of market conditions, including periods of financial stability and turbulence, thereby providing a robust foundation for evaluating the predictive efficacy of WDs of PH graphs in forecasting stock realized volatility as proposed by the TTD theory.

The dataset's RV measurements are based on high-frequency data within the day, namely 5-min data, sourced from the LOBSTER database. This database is renowned for its accuracy in providing limit order book data, ensuring the reliability and consistency of the RV assessments. The calculation of RV metrics, on the other hand, was conducted using the approach introduced [48]. For further information on this technique, refer to [48].

Additionally, a table of the considered stocks, together with a detailed statistical summary of their daily 5-min RV figures, is provided in A. The table includes a detailed array of statistical data such as the mean, median, and standard deviation, among other crucial statistical measures, offering a preliminary insight into the volatility characteristics of each stock included in the study.

Lastly, concerning the estimation of PH diagrams and WD values for the 80 stocks together, the algorithm proposed by Souto [30] is used. In essence, this algorithm estimates PH diagrams using last business month's returns of all considered stocks, yields one PH diagram per day, and estimates the WD value for a certain day as the WD of the PH diagram of that certain day and the PH diagram of the preceding day.

3.2. Linear regression analysis

This subsection delineates the linear regression framework adopted to empirically investigate the predictive power of WDs in forecasting next-day stock realized volatility, something predicted by the TTD theory [30,31]. Grounded in the Heterogeneous Autoregressive (HAR) model as proposed by Corsi [49], our study extends this model to incorporate WDs as a novel explanatory variable, alongside a suite of control variables, to assess their collective impact on realized volatility.

The augmented HAR model, henceforth denoted as HAR-WD, extends the traditional HAR model by incorporating WDs, alongside a carefully curated set of control variables, to capture the multifaceted influences on stock realized volatility. The model is specified as:

$$RV_{t+1} = \beta_0 + \beta_1 RV_t + \beta_2 RV_t^{(w)} + \beta_3 RV_t^{(m)} + \gamma WD_t + \sum_{i=1}^{k} \delta_i CV_{i,t} + \epsilon_{t+1}, \quad (1)$$

where RV_{t+1} denotes the realized volatility at time $t+1$, RV_t, $RV_t^{(w)}$, and $RV_t^{(m)}$ represent the daily, weekly, and monthly realized volatilities, respectively, and WD_t is the Wasserstein Distance at time t. The term $\sum_{i=1}^{k} \gamma_i CV_{i,t}$ captures the influence of k control variables selected based on theoretical relevance and empirical validation, with ϵ_{t+1} representing the error term.

Incidentally, we check the assumptions underlying linear regression are upheld. This involves checking whether the assumption of the linear regression theory are met and utilizing only the results of the stocks that meet these assumptions (unless if only the homoskedasticity of the residuals assumption is not met, then the Estimated Generalized Least Squares (EGLS) method is employed instead of Ordinary Least Squares (OLS) method). Besides this approach, multicollinearity is checked with Variance Inflation Factor (VIF) and handled by using a basic feature selection, which was enough for this study given the considered control variables, by excluding variables with VIF values higher than 10 and that do not have a statistically significant T-value and/or were highly correlated with another control variable.

Moving to the control variables, initially, a broad array of control variables was considered, drawing from established literature to capture various market and financial dynamics [30,31,50,51]. These variables, along with their respective proxies, are outlined below while the data sources where the historical values for these variables can be found in Appendix B:

- Log of VIX close price and VIX close price, serving as a proxy for market volatility expectations [30,31,50,51].
- US dollar foreign exchange index value (DXY), reflecting the strength of the US dollar in global markets [50].
- American credit spread, proxied by the Term Premium on a 10 Year Zero Coupon Bond (THREEFYTP1), to capture the risk perception in credit markets [50].
- American term spread, represented by the difference between 10-Year Treasury Constant Maturity and 3-Month Treasury Constant Maturity (T10Y3M), to gauge the yield curve's shape [50].
- Treasury-EuroDollar (TED) rate, indicating the credit risk in the banking sector [51].
- Fama–French five factors, extending the original three-factor model to include RMW (Robust Minus Weak) and CMA (Conservative Minus Aggressive) factors, reflecting a broader spectrum of market anomalies [30,31].

Post the multicollinearity assessment and feature selection, the final set of control variables incorporated into the HAR-WD model includes:

$$RV_{t+1} = \alpha + \beta RV_t + \gamma WD_t + \delta_1 \Delta CS_{t-1} + \delta_2 DXY_{t-1} + \delta_3 TED_{t-1} + \sum_{k=1}^{5} \delta_{3+k} FF5_{k,t-1} + \epsilon_{t+1}, \quad (2)$$

where ΔCS_{t-1} denotes the lagged American credit spread, DXY_{t-1} the lagged US dollar foreign exchange index value, TED_{t-1} the lagged TED rate, and $FF5_{k,t-1}$ the lagged values of the Fama–French five factors. This refined model respects the assumptions behind the linear regression theory and do not contain strong multicollinearity. By implementing this model and performing a linear regression analysis, we aim to evaluate to what extent one of the implications of the TTD theory, namely the statistically significant predictive power of WD lagged values for realized volatility [30,31], holds for individual stocks.

3.3. Granger causality framework

The Granger causality approach constitutes the second pivotal methodology in our exploration of the TTD theory and its predictions concerning the relationship between WD values and next-day stock realized volatility. Granger causality, a cornerstone in econometric literature [52–59], assesses the predictive ability of one time series over another, thereby enabling the inference of potential causal relationships within temporal data sequences [60]. Our application of this methodology is twofold, encompassing both linear and nonlinear paradigms since the TTD theory states that there is only a strong positive relationship between WD values and next-day stock realized volatility close to volatile periods [30,31]. Hence, nonlinear models would be able to capture this nonlinear relationship better than linear models, albeit linear models ought to be able to capture this relationship partially. Thus, the use of linear models has also the objective to compare the gain in predictive power with the addition of WD as an exogenous variable of the linear model and nonlinear model; if the gain in forecasting accuracy for the nonlinear model is considerably higher than for the linear model, this is also another evidence that the TTD theory is likely to be correct regarding the aforementioned implication of the theory.

The data split used for training and testing both linear and nonlinear models is 70%/30%. This division follows standard forecasting practices, ensuring enough model training and reliable performance evaluation [61]. Additionally, four error measures are used to assess the forecasting accuracy of the models in the testing sample: Root Mean Square Error (RMSE), Mean Absolute Error (MAE), Quasilikelihood (QLIKE), and Mean Percentage Absolute Error (MAPE). These metrics are defined as follows:

$$\text{RMSE} = \sqrt{\frac{1}{s \times n} \sum_{j=1}^{s} \sum_{i=1}^{n} (y_{i,j} - \hat{y}_{i,j})^2} \tag{3}$$

$$\text{MAE} = \frac{1}{s \times n} \sum_{j=1}^{s} \sum_{i=1}^{n} \left| y_{i,j} - \hat{y}_{i,j} \right| \tag{4}$$

$$\text{QLIKE} = \frac{1}{s \times n} \sum_{j=1}^{s} \sum_{i=1}^{n} \left(\frac{y_{i,j}}{\hat{y}_{i,j}} - \log\left(\frac{y_{i,j}}{\hat{y}_{i,j}}\right) - 1 \right) \tag{5}$$

$$\text{MAPE} = \frac{1}{s \times n} \sum_{j=1}^{s} \sum_{i=1}^{n} \left| \frac{y_{i,j} - \hat{y}_{i,j}}{y_{i,j}} \right| \tag{6}$$

where $y_{i,j}$ is the actual observation, $\hat{y}_{i,j}$ the forecasted value, n the total observations, and s the number of stocks. Together, these measures offer a complete evaluation of the forecasting power of the models [62,63].

In the realm of linear models, we employ the HAR model, as delineated by Corsi [49] and its augmented form with the incorporation of WD as an external variable. This extension aims to capture the linear predictive influence of WD on stock realized volatility, adhering to the traditional Granger causality framework that evaluates the statistical significance of added predictors. Eqs. (7) and (8) present the original HAR model and the HARX model respectively [49]:

$$RV_{t+1} = \beta_0 + \beta_1 RV_t + \beta_2 RV_t^{(w)} + \beta_3 RV_t^{(m)} + \epsilon_{t+1}, \tag{7}$$

$$RV_{t+1} = \beta_0 + \beta_1 RV_t + \beta_2 RV_t^{(w)} + \beta_3 RV_t^{(m)} + \gamma W D_t + \epsilon_{t+1}, \tag{8}$$

To transcend the limitations of linear assumptions and capture the positive nonlinear relationship between WD values and next-day stock realized volatility as proposed by the TTD theory [30,31], we incorporate nonlinear models through the cutting-edge NBEATSx neural network [64]. This model is employed in two configurations: one utilizing historical values of stock's realized volatility, henceforth named NBEATSx, and another extending the input space to include WD values, henceforth named NBEATSx-WD. The choice of the NBEATSx model over other nonlinear models is motivated by its superiority over other models in various forecasting tasks [64–66], including stock realized volatility forecasting [67]. To ensure sparsity of this paper, we opt to not mathematically and conceptually explain the architecture behind the NBEATSx model and refer readers interested in this architecture to [64].

The nonlinear nature of these models necessitates a departure from conventional Granger causality testing [60], leading to the adoption of the Diebold–Mariano (DM) test, initially devised by Diebold and Mariano [68] and improved by Harvey et al. [69]. This test evaluates the null hypothesis of equal predictive accuracy between models, enabling us to ascertain the incremental predictive value of WD in a nonlinear context. This adaptation is crucial for evaluating the TTD theory's premise that WD values, particularly during financially turbulent periods, hold enhanced predictive power for stock realized volatility. It is worth mentioning that the DM test is done for each considered error metric and stock individually for a more granular Granger causality testing while the p-value threshold is the standard threshold of 0.05.

To specifically address the TTD theory's implications, we also focus our analysis on the top ten percentile of trading days characterized by elevated market realized volatility. This selective approach allows us to scrutinize the theory's assertion that proximity to volatile financial periods magnifies the predictive relevance of WD, providing a nuanced understanding of its utility in forecasting stock realized volatility under stress conditions [30,31]. This comprehensive Granger causality framework, encompassing both linear and nonlinear models and tailored to the idiosyncrasies of financial market data, allows us to rigorously test the TTD theory. By evaluating the predictive enhancement offered by WD, particularly during periods of financial turbulence, we effectively put the TTD theory to the test for individual stocks.

Lastly, in the context of nonlinear models, the task of ascertaining the most suitable hyperparameters entails a rigorous and systematic exploration, encompassing a dedicated validation phase. During this validation phase, a portion equivalent to 28.5% of the training dataset is set aside for the purpose of fine-tuning the considered hyperparameters of the NBEATSx model, which can be found in Appendix C. This meticulous procedure entails the execution of a total of 40 distinct trials, each probing diverse hyperparameter configurations, and an additional set of 20 trials dedicated exclusively to the identification of the optimal random seed for maximal effectiveness. Finally, the optimal hyperparameters for NBEATSx and NBEATSx-WD can be found in Appendix D.

3.4. SHAP values

In our quest to empirically validate the TTD Theory, the third and concluding methodological facet employs SHAP (SHapley Additive exPlanations) values [70] to elucidate the impact of WD on the predictability of next-day stock realized volatility. SHAP values, rooted in cooperative game theory, offer a powerful framework for interpreting complex machine learning models by quantifying the contribution of each feature to the model's prediction for a given observation [70]. This interpretability tool has gained widespread recognition in machine learning literature for its ability to provide transparent and comprehensible explanations of model predictions, thereby bridging the gap between advanced machine learning techniques and practical decision-making [71–79].

The core idea of SHAP values hinges on the Shapley value, a concept that allocates payouts to players based on their contribution to the total payoff of the coalition they form. The Shapley value for a player (independent variable in our context) is computed as the average marginal contribution of this independent variable across all possible sets of considered independent variables for the model. Mathematically, the Shapley value ϕ_i for feature i in a coalition of N features is defined as [70]:

$$\phi_i(v) = \sum_{S \subseteq N \setminus \{i\}} \frac{|S|!(|N| - |S| - 1)!}{|N|!} \left(v(S \cup \{i\}) - v(S)\right), \tag{9}$$

where $v(S)$ represents the prediction function's value for a subset of features S, and $v(S \cup \{i\})$ denotes the value of the function when feature i is added to the subset S. The term $\frac{|S|!(|N|-|S|-1)!}{|N|!}$ ensures an equitable distribution, accounting for the number of permutations that include feature i in a coalition of size $|S|$. In the specific context of forecasting stock realized volatility using machine learning models, SHAP values offer a nuanced understanding of how lagged values of for instance realized volatility and WD influence the forecast. Consider a model predicting next-day volatility RV_{t+1} based on features $\{RV_t, RV_{t-1}, \ldots, WD_t\}$:

$$\hat{RV}_{t+1} = f(RV_t, RV_{t-1}, \ldots, WD_t), \tag{10}$$

where f represents the predictive model. The SHAP value for WD_t, for instance, quantifies the marginal contribution of the WD feature to the difference between the forecasted volatility $\hat{RV}_{t+1}$ and the average forecast over all data points. This insight is invaluable, especially when evaluating the TTD theory's assertion regarding the predictive significance of WD in proximity to volatile financial periods [30,31].

Table 1
Linear regressions results using Eq. (2).

Metric	Value
Number of stocks where EGLS was used instead of OLS due to heteroscedasticity	79 (out of 80)
Number of stocks where the residuals autocorrelation assumption was not met	1 (out of 80)
R^2	73.43% ± 5.5%
Adjusted R^2	73.50% ± 5.52%
Number of stocks where F-statistics p-value was below 0.01	79 (out of 79)
WD (t−1) coefficient value	0.0041 ± 0.0004
Number of stocks where T-statistics p-value for WD (t−1) was below 0.01	79 (out of 79)

Presented values for R^2, Adjusted R^2, and WD (t−1) coefficient value have the following format: mean value ± standard deviation value.

Visualizing these SHAP values, particularly through scatter plots with WD values on the X-axis and SHAP values on the Y-axis, elucidates the relationship between WD and its impact on volatility forecasts. Such visualizations can confirm or refute theoretical predictions of the TTD theory.

For this analysis, we employ the XGBoost (eXtreme Gradient Boosting) algorithm [80], due to its predictive power and compatibility with the 'shap' Python library (the Python library used in this study for the estimation of SHAP values). To ensure sparsity, this paper does not delve into the XGBoost's architecture and refers readers interested in it to Chen and Guestrin [80]. Consistent with the Linear Regression Analysis, the input variables for the XGBoost model include the same control variables found in Eq. (2), and, crucially, the WD values. This consistency ensures a harmonized basis for comparison across our methodological approaches. Our approach involves conducting separate regressions for each stock using the XGBoost model, followed by the computation of SHAP values for the WD variable. This individualized analysis allows for a nuanced understanding of the WD's predictive influence across different stocks. To synthesize these insights, we compute the mean SHAP values for the WD variable, facilitating a consolidated view of its impact. The culmination of our SHAP value analysis is a scatter plot that visualizes the relationship between WD values (X-Axis) and their corresponding SHAP values (Y-Axis).

This visualization strategy is designed to test the TTD theory's assertion regarding the behavior of the importance of WD values (here represented by SHAP values) for RV forecasting in relation to WD magnitudes. According to the theory, for WD values below the around 90th-percentile threshold, SHAP values are expected to exhibit a random distribution around zero, indicative of the WD's negligible predictive value in these ranges [30,31]. Conversely, for WD values surpassing this threshold, SHAP values should manifest as positive and significant, underscoring the enhanced predictive utility of WD in forecasting stock realized volatility during periods proximal to financial turbulence [30,31].

4. Empirical experimentation

4.1. Linear regression analysis

Table 1 presents the aggregated main results of the linear regressions for all considered stocks using Eq. (2), while Tables 2 and 3 present the coefficient values and their standard deviations for the explanatory variables other than WD (t − 1), as well as the significance of the T-statistics p-values for these explanatory variables, respectively.

It can be seen that virtually all linear regressions possess heteroscedasticity in their residuals, demanding the use of EGLS instead of OLS. Interestingly, the only model that does not have heteroscedasticity in its residuals is also the same model where the residuals autocorrelation assumption is not met. As a result of the latter fact, this model is not considered for the henceforth analysis of the linear regressions results. The R^2 and Adjusted R^2 are relatively high, albeit there exists a considerably high variation among the stocks. Given the Anderson–Darling test statistic result of 0.580 for both variables and assuming that

Table 2
Other explanatory variables coefficient values and their standard deviations.

Variable	Coefficient value
D (t−1) coefficient value	0.7495 ± 0.0452
Mkt_RF (t−1) coefficient value	−0.0002 ± 0.0001
SMB (t−1) coefficient value	−0.0001 ± 0.0001
HML (t−1) coefficient value	−4.8e−05 ± 8.7e−05
RMW (t−1) coefficient value	0.0002 ± 0.0002
CMA (t−1) coefficient value	0.0001 ± 0.0002
Credit spread (t−1) coefficient value	0.0001 ± 0.0003
TEDRATE (t−1) coefficient value	0.0014 ± 0.0005
Dolar index value (t−1) coefficient value	−4e−06 ± 2.6e−05

Table 3
Number of stocks where T-statistics was significant for other explanatory variables.

Variable	p-value = 0.05	p-value = 0.01
D (t−1)	79 (out of 79)	79 (out of 79)
Mkt_RF (t−1)	72 (out of 79)	66 (out of 79)
SMB (t−1)	21 (out of 79)	14 (out of 79)
HML (t−1)	8 (out of 79)	0 (out of 79)
RMW (t−1)	21 (out of 79)	7 (out of 79)
CMA (t−1)	5 (out of 79)	0 (out of 79)
Credit spread (t−1)	22 (out of 79)	13 (out of 79)
TEDRATE (t−1)	79 (out of 79)	79 (out of 79)
Dollar index value (t−1)	31 (out of 79)	22 (out of 79)

they are random variables, we can construct 99.7% confidence intervals using the normal distribution as a basis. As a result, we can claim that our linear regression model will likely have a R^2 and Adjusted R^2 between 56.93% and 89.93%, and 56.94% and 90.06% respectively for a given American stock, showing the heterogeneity present in the considered sample.

Incidentally, all linear regressions present a F-statistics p-value below the conservative threshold of 0.01, showing the all considered models pass the standard F-statistics check. Last but not least, all linear regressions present a T-statistics p-value for WD (t − 1) below the conservative threshold of 0.01 and all the coefficients of WD (t − 1) are positive, showing that the prediction of the TTD theory regarding the significant and positive relationship between WD values and next day's realized volatility is correct. Consequently, not only do the results of the Linear Regression Analysis in this study not allow us to falsify the generalization of the TTD theory for individual stocks, but it also serves as evidence that the TTD theory could likely be correct, albeit further analysis with the Granger causality and SHAP values methodologies are needed to affirm this with certainty.

Lastly, when considering the results present in Tables 2 and 3, the significance of the other explanatory variables, and thus their importance for a proper linear regression analysis, becomes empirically clear, with the exception of HML (t − 1) and CMA (t − 1). However, an in-depth analysis of and financial economic explanation for the coefficient values is omitted to ensure the sparsity of this paper and due to the fact that it lies outside the scope of this paper.

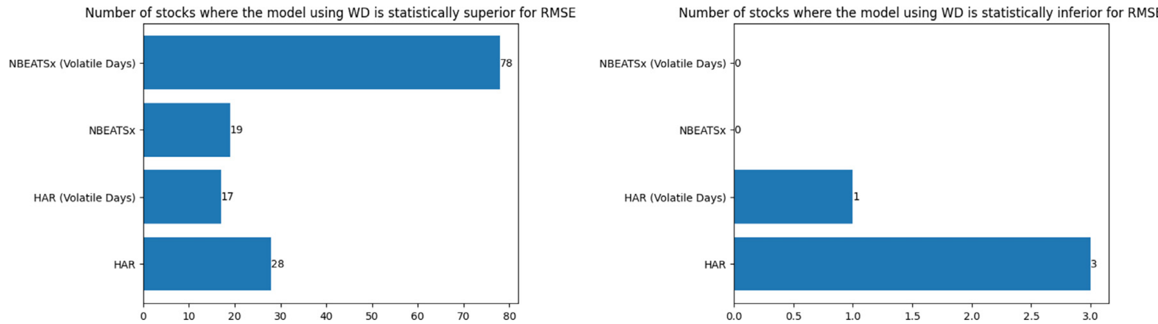

Fig. 7. DM tests results for RMSE.

Table 4
Error measures relative results.

Model	RMSE	MAE	QLIKE	MAPE
HARX (full testing sample)	99.59%	100.03%	99.32%	100.53%
NBEATSx-WD (full testing sample)	96.37%	99.97%	95.40%	103.16%
HARX (10th most volatile percentile of testing sample)	99.10%	99.64%	96.69%	100.56%
NBEATSx-WD (10th most volatile percentile of testing sample)	88.68%	90.00%	78.55%	92.16%

Presented values are relative values, in the sense that they are divided by the error metrics values of the models without WD (t−1) in order to facilitate the analysis and interpretation of the results.

4.2. Granger causality framework

The error metrics relative results for both linear and nonlinear models and considering the full testing sample or only the top 10th most volatile percentile of the testing sample can be found in Table 4. It is worth mentioning that the present values are relative values, meaning they are normalized by dividing them by the error metrics values of the models without WD (t − 1). This normalization facilitates the analysis and interpretation of the results. Mathematically, this can be expressed as:

$$\text{Relative Value} = \frac{\text{Value with WD } (t-1)}{\text{Value without WD } (t-1)}$$

This formula ensures that the values are easier to compare and interpret by providing a consistent basis for evaluation.

It can be seen that for the linear models (HAR and HARX), there is barely no improvement in the predictive power with the addition of WD (t − 1) information for the full testing sample and to some extent for the 10th most volatile percentile of the testing sample, with the exception of the QLIKE error measure. Regarding the nonlinear model (NBEATSx and NBEATSx-WD), on the other hand, there is a more clear improvement in the predictive accuracy with the addition of WD (t − 1) information, especially for the 10th most volatile percentile of the testing sample. This is exactly what the TTD theory predicts, namely that there exists a significant nonlinear relationship between WD values and next day's realized volatility, which implies that the addition of WD (t − 1) information for forecasting models would be beneficial especially for nonlinear models and during volatile periods. Despite these primary results, statistical testing with the DM test is still required to validate the results and conclusions from Table 4.

Fig. 7 depicts the aggregated results of DM tests for RMSE. It is worth noting that the results shown in Fig. 7 and subsequent figures in this chapter are based on the number of stocks where the *p*-value for the DM test is below the standard *p*-value threshold of 0.05. Interestingly, it can be seen that the incorporation of WD (t − 1) information to both the linear and nonlinear models led to a statistical superiority of the models in forecasting accuracy, with the nonlinear model following the prediction of the TTD theory of the model with WD (t − 1) performing better in volatile times while the linear model not. However, this can also be explained by another implication of the TTD theory, namely the nonlinear relationship of WD values and next day's realized volatility, which needless to say can only be properly captured by nonlinear models.

The DM tests results for MAE can be seen in Fig. 8. Now, a clear and statistically significant improvement of forecast precision is observed only for the nonlinear model and during volatile periods, as predicted by the TTD theory.

Moving to the results of the DM tests for QLIKE, which can be found in Fig. 9, the situation is almost identical to the DM tests results for RMSE. Hence, the same conclusions drawn for RMSE are applicable here.

Lastly, Fig. 10 shows the results the DM tests for MAPE. Interestingly, in both cases the models without WD (t − 1) information perform statistically better considering the whole testing sample. Yet, when considering volatile periods, the incorporation of WD (t − 1) information leads to a superiority of the nonlinear model and an equality for the linear model. The superiority of the models without WD (t − 1) information, when considering the whole testing sample, can presumably be explained by the fact that the MAPE error measure considers the relative error (i.e., the error normalized by the real value), which makes this error metric to treat errors in volatile and non-volatile periods with the same weight. Therefore, not only is the increase in forecasting power through the addition of WD (t − 1) information not perceived when considering the whole testing sample, but also the incorporation of WD (t − 1) information has a negative impact on the forecasting power of the models during non-volatile periods. This is explained by the TTD theory's implication of the nonlinear positive relationship between WD values and next day's realized volatility, which is only present during periods preceding (and during as well) volatile times. Thus, the models using WD (t − 1) information likely detect and utilize a spurious relationship between WD values and next day's realized volatility for non-volatile periods during the training stage, which lead to a relatively poorer performance of these models for predictions for non-volatile periods in the testing sample. In conclusion, although the results presented in Fig. 10 might at first seem to be against the predictions of the TTD theory, after a good look, they are actually evidence for the TTD theory.

4.3. SHAP values

Fig. 11 shows a scatter plot with a histogram of the normalized WD (t − 1) values in the X-axis and SHAP values for WD (t − 1) in the Y-Axis. As predicted by the TTD theory, the importance of the relationship between WD values and next day's realized volatility is non-existent and becomes positive and significant for the top percentiles of WD

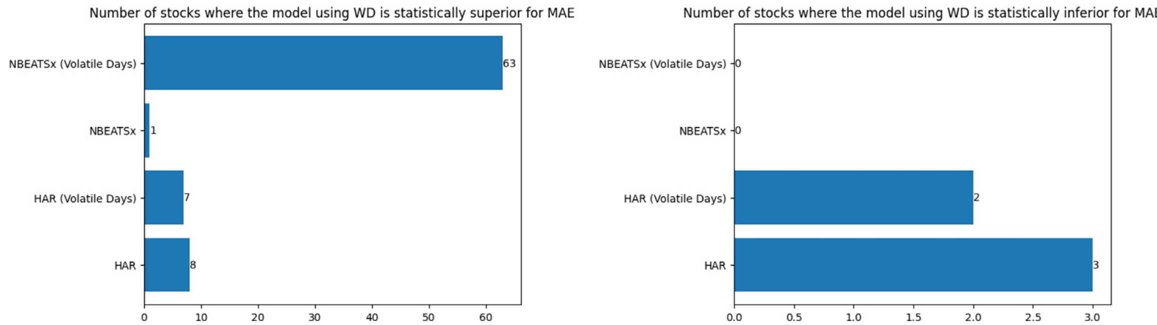

Fig. 8. DM tests results for MAE.

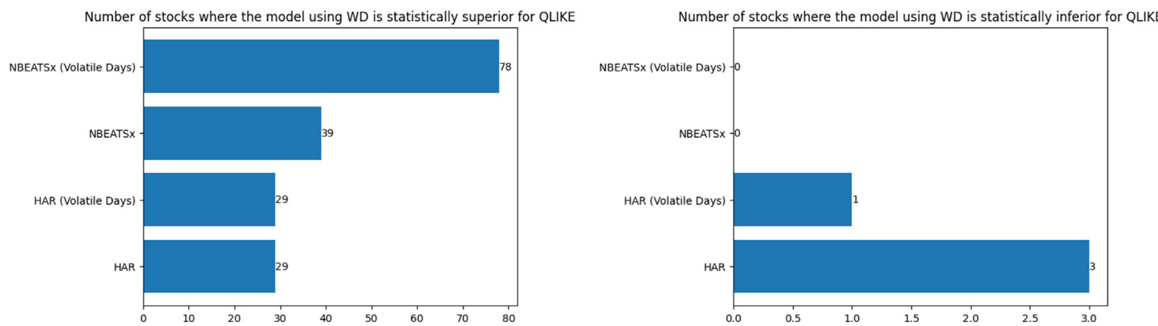

Fig. 9. DM tests results for QLIKE.

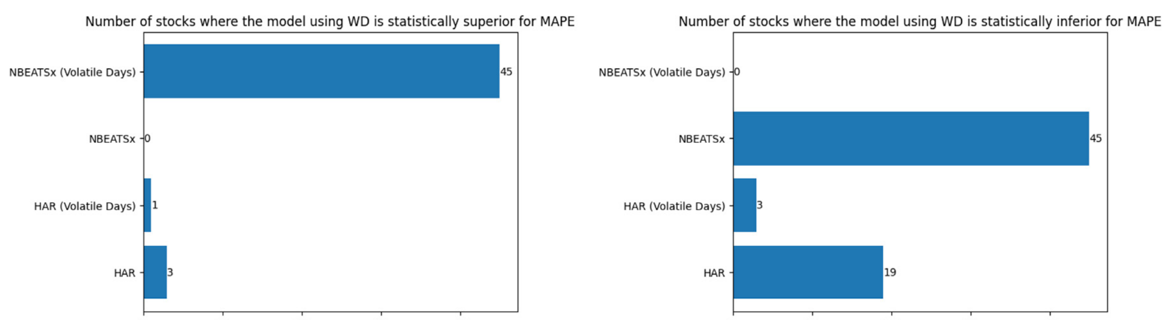

Fig. 10. DM tests results for MAPE.

values. This can be seen by the fact that for the greatly majority of WD values (values roughly below the 90th percentile threshold), the SHAP values for WD ($t-1$) are centered between 0 and approximately distributed as a normal distribution, showing that the estimated SHAP values are likely noise and there is indeed no relationship between WD values and next day's realized volatility. Incidentally, this is also an evidence for the proposed explanation for the results of Fig. 10. On the other hand, for a small minority of WD values (values roughly above the 90th percentile threshold), the SHAP values for WD ($t-1$) are clearly positive, demonstrating the positive and significant relationship between WD values and next day's realized volatility for the top percentiles of WD values.

Table 5
Methods used to test the TTD theory and their respective conclusions.

Method	Conclusion
Linear regression analysis	Significant positive relationship between WD values and next day's realized volatility, as predicted by the TTD theory.
Granger causality framework	Significantly improvement in predictive accuracy for nonlinear models, especially during volatile periods, as predicted by the TTD theory.
SHAP values	Positive and significant relationship between WD values and next day's realized volatility for top percentiles of WD values, as predicted by the TTD theory.

4.4. Summary

Table 5 summarizes the methods used to test the TTD theory and their respective conclusions. It can observed that each method provided compelling evidence supporting the theory.

Regarding the linear regression analysis, the analysis revealed a significant positive relationship between WD values and the next day's realized volatility. This result aligns with the TTD theory's prediction that higher WD values are associated with increased volatility, confirming the theory's applicability at the individual stock level. Moving to the Granger causality framework, the framework showed a notable improvement in predictive accuracy for nonlinear models, particularly

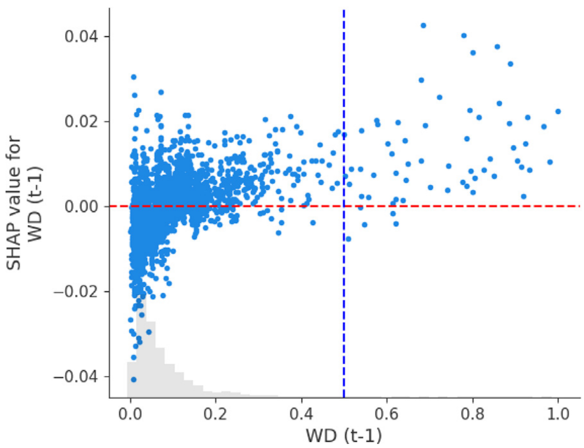

Fig. 11. Scatter plot of WD (t − 1) SHAP values and WD (t − 1) values.

during volatile periods. This finding supports the TTD theory's assertion of a nonlinear relationship between WD values and subsequent realized volatility. Finally, the SHAP values analysis demonstrated a positive and significant relationship between WD values and next day's realized volatility for the top percentiles of WD values. This result further substantiates the TTD theory, highlighting the importance of WD values in predicting volatility, especially for extreme values, as predicted by the theory.

Collectively, the results from these methods provide strong evidence in favor of the TTD theory. They demonstrate that the theory not only holds true for individual stocks but also generalizes well to high dimensions, involving numerous stocks. This reinforces the robustness and broad applicability of the TTD theory in different market conditions and across various financial instruments.

5. Research limitations

While the empirical results indicate a significant relationship between WD and realized volatility, this finding should be approached with caution. The linear regression analysis demonstrates that WD (t − 1) has a positive and statistically significant impact on next-day realized volatility. However, this relationship may not fully capture the complexity of market dynamics. Alternative explanations for the observed relationship could include omitted variable bias or other latent factors influencing both WD and volatility. For instance, market microstructure effects or varying liquidity conditions might also play roles that were not explicitly modeled in this study. Additionally, the nonlinear Granger causality framework further supports the TTD theory's prediction that the relationship between WD and realized volatility intensifies during volatile periods. Nonetheless, the limited improvement in predictive power for linear models incorporating WD suggests that the full explanatory power of WD may only be realized in more complex, nonlinear models.

Incidentally, this study acknowledges several critical assumptions that underpin the analysis, including those related to heteroscedasticity. The extensive presence of heteroscedasticity in the residuals necessitated the use of Estimated Generalized Least Squares (EGLS) instead of Ordinary Least Squares (OLS) for 79 out of the 80 stocks analyzed. Although EGLS addresses heteroscedasticity, it introduces complexity and potential sensitivity to model specifications.

Another crucial assumption involves the linearity of the models used in the initial regression analysis. Given the evidence of nonlinearity in the relationship between WD and realized volatility, as highlighted by the improved performance of nonlinear models, the reliance on linear models may limit the scope of the findings. The nonlinear nature of the relationship suggests that further exploration with more sophisticated and nonlinear models could yield deeper insights. Moreover, the potential for sample selection bias and model specification errors must be considered. The dataset comprises stocks from the S&P 100 index, which may not be representative of the broader market. This limitation could restrict the generalizability of the findings. Additionally, the choice of control variables, while based on established literature, might omit other relevant factors, leading to omitted variable bias.

The discussion on assumptions and limitations emphasizes the need for cautious interpretation of the results. Future research could benefit from expanding the dataset to include a wider array of stocks and incorporating additional control variables to mitigate potential biases. Moreover, employing advanced econometric and machine learning techniques could provide a more nuanced understanding of the complex dynamics at play.

In summary, while the study provides evidence supporting the TTD theory's predictions, the limitations related to model assumptions, potential biases, and the inherent complexity of financial markets suggest that these findings should be interpreted as indicative rather than definitive. Further research is warranted to validate and extend these results in different contexts and with more sophisticated methodologies.

6. Conclusion

This study embarked on an empirical journey to explore the applicability of the Topological Tail Dependence (TTD) theory to individual stock realized volatility, employing a multifaceted methodological approach encompassing linear regression analysis, Granger causality framework, and SHAP value analysis. The findings unveil that the TTD theory can successfully be generalized to individual stocks and in high dimensions, allowing for the use of the temporal moving Wasserstein Distance (WD) estimations of Persistent Homology (PH) diagrams to better model and forecast stock realized volatility and volatile periods.

The Linear Regression Analysis revealed a significant and positive relationship between WD and subsequent day's realized volatility, lending empirical support to the TTD theory's prediction of the significant relationship between WD and next day's realized volatility. The Granger causality approach, on the other hand, further nuanced our understanding, particularly through the lens of nonlinear models like NBEATSx, which demonstrated a marked improvement in predictive accuracy upon the inclusion of WD, especially during periods of heightened volatility. This finding resonates with the TTD theory's assertion of a significant positive nonlinear relationship between WD and future realized volatility, suggesting that WD's predictive utility is only present preceding and under turbulent market conditions. Finally, the SHAP value analysis provided a granular view of this relationship, revealing that the impact of WD on volatility predictions is predominantly pronounced for values in the upper percentiles, aligning with the TTD theory's propositions. This observation not only corroborates the theory's validity but also highlights the importance of considering topological features in volatility forecasting, particularly in the context of volatile periods.

The practical implications of these findings are manifold. Firstly, the demonstrated relationship between WD and realized volatility provides a novel predictive tool for market participants. By incorporating WD into predictive models, financial analysts and traders can potentially improve the accuracy of their volatility forecasts, particularly during volatile market conditions. This enhancement in forecasting can lead to more informed trading strategies, better risk management, and improved portfolio optimization. Moreover, the ability to predict periods of heightened volatility with greater precision can aid in the development of dynamic hedging strategies, reducing the potential for significant financial losses during turbulent periods.

Additionally, the insights gleaned from this study open several avenues for future research. Extending the analysis to a broader array of financial instruments, including derivatives and fixed-income securities, could provide a more comprehensive understanding of the

Table 6
Summary statistics of 5-min realized volatility daily values.

Tickers	Mean	Std	Min	25%	50%	75%	Max
AAPL	1.32%	0.74%	0.27%	0.84%	1.12%	1.57%	6.08%
ABT	1.07%	0.51%	0.35%	0.75%	0.94%	1.22%	5.70%
ACN	1.15%	0.63%	0.37%	0.76%	0.96%	1.33%	7.28%
ADBE	1.42%	0.70%	0.40%	0.96%	1.24%	1.66%	6.64%
ADP	1.04%	0.57%	0.32%	0.70%	0.89%	1.18%	6.56%
AMGN	1.26%	0.55%	0.40%	0.90%	1.13%	1.46%	5.71%
AMT	1.27%	0.74%	0.43%	0.83%	1.05%	1.45%	7.17%
AMZN	1.57%	0.86%	0.33%	1.01%	1.36%	1.89%	7.71%
AXP	1.43%	1.05%	0.35%	0.80%	1.07%	1.63%	9.31%
BA	1.40%	0.85%	0.36%	0.88%	1.16%	1.61%	9.37%
BAC	1.75%	1.36%	0.32%	1.01%	1.34%	1.92%	11.45%
BDX	1.06%	0.50%	0.36%	0.74%	0.93%	1.22%	5.27%
BMY	1.20%	0.55%	0.29%	0.85%	1.07%	1.39%	5.43%
BSX	1.57%	0.81%	0.45%	1.07%	1.38%	1.83%	7.31%
C	1.80%	1.48%	0.39%	1.00%	1.35%	1.98%	15.64%
CAT	1.47%	0.79%	0.39%	0.97%	1.26%	1.70%	6.62%
CB	1.11%	0.76%	0.27%	0.66%	0.86%	1.27%	7.59%
CI	1.61%	1.01%	0.43%	1.01%	1.32%	1.81%	12.53%
CMCSA	1.34%	0.73%	0.34%	0.88%	1.15%	1.57%	6.84%
CME	1.48%	0.94%	0.43%	0.92%	1.17%	1.65%	8.21%
COP	1.53%	0.87%	0.40%	0.99%	1.31%	1.80%	8.50%
COST	1.07%	0.57%	0.31%	0.73%	0.92%	1.21%	5.32%
CRM	1.79%	0.89%	0.47%	1.20%	1.55%	2.15%	7.76%
CSCO	1.25%	0.65%	0.37%	0.84%	1.07%	1.45%	6.42%
CVS	1.29%	0.65%	0.39%	0.87%	1.10%	1.47%	6.02%
CVX	1.35%	0.79%	0.38%	0.85%	1.13%	1.57%	6.77%
D	0.94%	0.52%	0.27%	0.63%	0.80%	1.07%	5.11%
DD	1.37%	0.71%	0.37%	0.90%	1.17%	1.59%	6.46%
DHR	1.16%	0.60%	0.35%	0.78%	0.99%	1.32%	5.96%
DIS	1.25%	0.73%	0.34%	0.83%	1.07%	1.44%	7.38%
DUK	0.94%	0.49%	0.30%	0.63%	0.79%	1.06%	5.24%
FIS	1.18%	0.70%	0.39%	0.77%	0.98%	1.32%	7.74%
FISV	1.14%	0.63%	0.38%	0.76%	0.96%	1.30%	7.17%
GE	1.49%	0.85%	0.36%	0.93%	1.23%	1.73%	7.54%
GILD	1.37%	0.70%	0.39%	0.90%	1.16%	1.59%	6.75%
GOOGL	1.37%	0.72%	0.39%	0.90%	1.17%	1.60%	7.02%
GS	1.65%	1.03%	0.44%	1.02%	1.35%	1.90%	9.45%
HD	1.25%	0.67%	0.38%	0.84%	1.07%	1.43%	6.93%
HON	1.17%	0.63%	0.38%	0.80%	1.00%	1.31%	6.52%
IBM	1.21%	0.66%	0.36%	0.82%	1.04%	1.38%	6.89%
INTC	1.39%	0.73%	0.39%	0.90%	1.17%	1.62%	7.13%
INTU	1.27%	0.63%	0.39%	0.86%	1.10%	1.47%	6.13%
ISRG	1.58%	0.82%	0.47%	1.05%	1.35%	1.84%	6.78%
JNJ	0.97%	0.49%	0.31%	0.68%	0.83%	1.08%	5.44%
JPM	1.59%	1.09%	0.38%	0.93%	1.23%	1.79%	10.12%
KO	0.90%	0.48%	0.30%	0.63%	0.78%	1.00%	5.33%
LLY	1.23%	0.65%	0.38%	0.84%	1.06%	1.39%	6.90%
LMT	1.12%	0.61%	0.35%	0.76%	0.95%	1.26%	6.33%
LOW	1.30%	0.72%	0.35%	0.89%	1.11%	1.48%	7.23%
MA	1.39%	0.77%	0.38%	0.91%	1.17%	1.62%	7.41%
MCD	0.98%	0.54%	0.30%	0.67%	0.83%	1.10%	5.66%
MDT	1.10%	0.54%	0.36%	0.77%	0.96%	1.25%	5.96%
MMM	1.04%	0.58%	0.29%	0.68%	0.90%	1.22%	5.49%
MO	1.05%	0.55%	0.25%	0.72%	0.92%	1.20%	6.18%
MRK	1.13%	0.60%	0.35%	0.76%	0.96%	1.32%	5.49%
MS	1.90%	1.42%	0.44%	1.12%	1.48%	2.08%	15.72%
MSFT	1.20%	0.61%	0.34%	0.82%	1.04%	1.38%	5.44%
NFLX	2.15%	0.95%	0.60%	1.46%	1.94%	2.60%	8.48%
NKE	1.26%	0.65%	0.38%	0.86%	1.07%	1.42%	6.87%
NVDA	2.04%	0.98%	0.63%	1.35%	1.79%	2.44%	8.42%
ORCL	1.22%	0.64%	0.27%	0.81%	1.07%	1.43%	6.52%
PEP	0.89%	0.48%	0.25%	0.61%	0.76%	1.00%	5.17%
PFE	1.12%	0.54%	0.37%	0.76%	0.97%	1.29%	5.09%
PG	0.88%	0.47%	0.30%	0.62%	0.76%	0.99%	5.50%
PNC	1.54%	1.11%	0.40%	0.89%	1.17%	1.74%	11.58%
QCOM	1.39%	0.71%	0.32%	0.90%	1.22%	1.66%	6.38%
SBUX	1.35%	0.79%	0.42%	0.84%	1.11%	1.57%	7.84%
SO	0.97%	0.49%	0.34%	0.68%	0.85%	1.10%	5.86%
SYK	1.15%	0.59%	0.29%	0.78%	0.99%	1.32%	6.94%
T	1.05%	0.61%	0.29%	0.69%	0.87%	1.18%	5.53%
TGT	1.35%	0.78%	0.34%	0.87%	1.11%	1.53%	7.18%
TJX	1.34%	0.72%	0.40%	0.87%	1.11%	1.59%	7.32%
TMO	1.23%	0.61%	0.39%	0.84%	1.07%	1.41%	6.25%
TXN	1.36%	0.68%	0.41%	0.92%	1.19%	1.60%	6.89%
UNH	1.41%	0.83%	0.40%	0.88%	1.16%	1.60%	7.13%
UNP	1.39%	0.77%	0.37%	0.91%	1.18%	1.58%	6.66%
UPS	1.10%	0.60%	0.31%	0.71%	0.94%	1.31%	5.51%
USB	1.42%	1.07%	0.37%	0.79%	1.08%	1.63%	9.41%
VZ	1.03%	0.57%	0.31%	0.70%	0.88%	1.15%	5.70%
WFC	1.58%	1.23%	0.33%	0.85%	1.18%	1.80%	10.07%
WMT	0.96%	0.50%	0.34%	0.67%	0.82%	1.08%	5.09%

(*continued on next page*)

TTD theory's applicability across the financial spectrum. Exploring the integration of alternative topological estimations instead of WD, for instance, L^n norms of Persistent Landscapes, could yield more sophisticated models capable of better capturing the multifaceted nature of market dynamics. Moreover, the nuanced role of WD during volatile periods invites further investigation into the temporal aspects of topological dependence, potentially leading to dynamic modeling approaches that adapt to changing market conditions. Lastly, the application of advanced topological data analysis techniques, beyond PH, could uncover deeper insights into the structural intricacies of financial markets, offering novel perspectives on risk management and investment strategy formulation.

In conclusion, this research not only affirms the potential of the TTD theory in enhancing our understanding of stock volatility but also underscores the importance of topological considerations in financial modeling. The practical applications of these findings are significant, offering new tools and strategies for market participants to navigate volatility more effectively. The evidence presented herein, while supportive of the TTD theory, also highlights the complexity of financial markets and the need for continued innovation in analytical methodologies. As we advance the frontier of financial econometrics, the integration of topological data analysis (TDA) with traditional and machine learning approaches promises to enrich our toolkit for navigating the ever-evolving landscape of financial volatility.

Data and code availability

Data will be shared upon request. Regarding the code used in this study, the link to the GitHub repository where all Jupyter Notebooks used in this research can be found will be shared upon the publication of this study.

Declaration of competing interest

The authors declare that they have no known competing financial interests or personal relationships that could have appeared to influence the work reported in this paper.

Data availability

Data will be made available on request.

Declaration of Generative AI and AI-assisted technologies in the writing process

During the preparation of this work the author used ChatGPT in order to check the use of language in the manuscript and point out any spelling or grammatical errors. After using this tool, the author reviewed and edited the content as needed and takes full responsibility for the content of the publication.

Appendix A. Summary statistics of S&P100 dataset

See Table 6.

Table 7
Data sources of considered control variables.

Variable	Data source
VIX close price	Yahoo Finance API
DXY	MarketWatch
THREEFYTP1	FRED Economic Data
T10Y3M	FRED Economic Data
TED rate	FRED Economic Data
Fama–French five factors	Kenneth R. French Website

Table 8
NBEATSx hyperparameters search space.

Hyperparameters	Options
n_inputs	[3, 5, 10, 15, 21, 42, 84]
mlp_units	[[[712, 712], [712, 712]], [[512, 512], [512, 512]], [[250, 250], [250, 250]], [[100, 100], [100, 100]]]
epochs	[50, 100, 150, 250, 350, 450, 550, 650, 750]
learning_rate	[0.0005, 0.0001, 0.00005, 0.00001]
num_lr_decays	[5, 3, 2, 1]
scaler_type	["robust", "standard", "minmax"]
losses	[MSE(), MAE(), MQLoss(level = [80, 90]), DistributionLoss(distribution = 'StudentT', level = [80, 90])]
n_harmonics	[0, 0, 1, 1]
n_blocks	[[1, 1], [2, 2], [3, 3], [5, 5]]
n_polynomials	[0, 1, 0, 1]

Table 9
Optimal NBEATSx hyperparameters.

Hyperparameters	Optimal
n_inputs	[15]
mlp_units	[[512, 512], [512, 512]]
epochs	[450]
learning_rate	[0.00001]
num_lr_decays	[1]
scaler_type	["minmax"]
losses	[MQLoss(level = [80, 90])]
n_harmonics	[0]
n_blocks	[5, 5]
n_polynomials	[0]

Table 10
Optimal NBEATSx-WD hyperparameters.

Hyperparameters	Optimal
n_inputs	[3]
mlp_units	[[100, 100], [100, 100]]
epochs	[750]
learning_rate	[0.00005]
num_lr_decays	[2]
scaler_type	["standard"]
losses	[DistributionLoss(distribution = 'StudentT', level = [80, 90])]
n_harmonics	[0]
n_blocks	[2, 2]
n_polynomials	[0]

Appendix B. Data sources of considered control variables

See Table 7.

Appendix C. Hyperparameters search space for NBEATSx and NBEATSx-WD

See Table 8.

Appendix D. Optimal hyperparameters for NBEATSx and NBEATSx-WD

See Tables 9 and 10.

References

[1] D. Das, P. Kayal, M. Maiti, A K-means clustering model for analyzing the bitcoin extreme value returns, Decis. Anal. J. (ISSN: 2772-6622) 6 (2023) 100152, http://dx.doi.org/10.1016/j.dajour.2022.100152.

[2] J.K. Afriyie, K. Tawiah, W.A. Pels, S. Addai-Henne, H.A. Dwamena, E.O. Owiredu, S.A. Ayeh, J. Eshun, A supervised machine learning algorithm for detecting and predicting fraud in credit card transactions, Decis. Anal. J. (ISSN: 2772-6622) 6 (2023) 100163, http://dx.doi.org/10.1016/j.dajour.2023.100163.

[3] P. Bennett, L. Wei, Market structure, fragmentation, and market quality, J. Financial Mark. (ISSN: 1386-4181) 9 (1) (2006) 49–78, http://dx.doi.org/10.1016/j.finmar.2005.12.001.

[4] N. Cetorelli, M. Gambera, Banking market structure, financial dependence and growth: International evidence from industry data, J. Finance (ISSN: 1540-6261) 56 (2) (2001) 617–648, http://dx.doi.org/10.1111/0022-1082.00339.

[5] G.-H. Moon, W.-C. Yu, Volatility spillovers between the US and China stock markets: Structural break test with symmetric and asymmetric GARCH approaches, Glob. Econ. Rev. (ISSN: 1744-3873) 39 (2) (2010) 129–149, http://dx.doi.org/10.1080/1226508x.2010.483834.

[6] B.T. Ewing, F. Malik, Volatility spillovers between oil prices and the stock market under structural breaks, Glob. Finance J. (ISSN: 1044-0283) 29 (2016) 12–23, http://dx.doi.org/10.1016/j.gfj.2015.04.008.

[7] R. Jung, R. Maderitsch, Structural breaks in volatility spillovers between international financial markets: Contagion or mere interdependence? J. Bank. Financ. (ISSN: 0378-4266) 47 (2014) 331–342, http://dx.doi.org/10.1016/j.jbankfin.2013.12.023.

[8] M. Bonato, O. Cepni, R. Gupta, C. Pierdzioch, Forecasting the realized volatility of agricultural commodity prices: Does sentiment matter? J. Forecast. (ISSN: 1099-131X) (2024) http://dx.doi.org/10.1002/for.3106.

[9] H.G. Souto, Time series forecasting models for S&P 500 financial turbulence, J. Math. Finance (ISSN: 2162-2442) 13 (01) (2023) 112–129, http://dx.doi.org/10.4236/jmf.2023.131007.

[10] C.M. Mesquita, C.A. Valle, A.C.M. Pereira, Scenario generation for financial data with a machine learning approach based on realized volatility and copulas, Comput. Econ. (2023) http://dx.doi.org/10.1007/s10614-023-10387-2.

[11] A. Atkins, M. Niranjan, E. Gerding, Financial news predicts stock market volatility better than close price, J. Finance Data Sci. (ISSN: 2405-9188) 4 (2) (2018) 120–137, http://dx.doi.org/10.1016/j.jfds.2018.02.002.

[12] M. Bonato, O. Cepni, R. Gupta, C. Pierdzioch, Forecasting realized volatility of international REITs: The role of realized skewness and realized kurtosis, J. Forecast. (ISSN: 1099-131X) 41 (2) (2021) 303–315, http://dx.doi.org/10.1002/for.2813.

[13] M. Bašta, P. Molnár, Oil market volatility and stock market volatility, Finance Res. Lett. (ISSN: 1544-6123) 26 (2018) 204–214, http://dx.doi.org/10.1016/j.frl.2018.02.001.

[14] M. Liu, W.-C. Choo, C.-C. Lee, C.-C. Lee, Trading volume and realized volatility forecasting: Evidence from the China stock market, J. Forecast. (ISSN: 1099-131X) 42 (1) (2022) 76–100, http://dx.doi.org/10.1002/for.2897.

[15] X. Tang, Y. Song, X. Jiao, Y. Sun, On forecasting realized volatility for bitcoin based on deep learning PSO–GRU model, Comput. Econ. (2023) http://dx.doi.org/10.1007/s10614-023-10392-5.

[16] C. Zhang, Y. Zhang, M. Cucuringu, Z. Qian, Volatility forecasting with machine learning and intraday commonality, J. Financ. Econom. (ISSN: 1479-8417) 22 (2) (2024) 492–530, http://dx.doi.org/10.1093/jjfinec/nbad005.
[17] H.G. Souto, Charting new avenues in financial forecasting with TimesNet: The impact of intraperiod and interperiod variations on realized volatility prediction, Expert Syst. Appl. (ISSN: 0957-4174) 255 (2024) 124851, http://dx.doi.org/10.1016/j.eswa.2024.124851.
[18] R.L. D'Ecclesia, D. Clementi, Volatility in the stock market: ANN versus parametric models, Ann. Oper. Res. (ISSN: 1572-9338) 299 (1–2) (2019) 1101–1127, http://dx.doi.org/10.1007/s10479-019-03374-0.
[19] J. Li, The comparison of LSTM, LGBM, and CNN in stock volatility prediction, in: Advances in Economics, Business and Management Research, in: icfied-22, Atlantis Press, (ISSN: 2352-5428) 2022, http://dx.doi.org/10.2991/aebmr.k.220307.147.
[20] A. Vidal, W. Kristjanpoller, Gold volatility prediction using a CNN-LSTM approach, Expert Syst. Appl. (ISSN: 0957-4174) 157 (2020) 113481, http://dx.doi.org/10.1016/j.eswa.2020.113481.
[21] Y. Zhang, Stock volatility prediction with hybrid model of FFNN and lightgbm, in: 2022 7th International Conference on Intelligent Computing and Signal Processing, ICSP, 2022, pp. 750–754.
[22] A. Bucci, Realized volatility forecasting with neural networks, J. Financ. Econom. (ISSN: 1479-8417) 18 (3) (2020) 502–531, http://dx.doi.org/10.1093/jjfinec/nbaa008.
[23] B. Lei, B. Zhang, Y. Song, Volatility forecasting for high-frequency financial data based on web search index and deep learning model, Mathematics (ISSN: 2227-7390) 9 (4) (2021) 320, http://dx.doi.org/10.3390/math9040320.
[24] M. Gidea, Topological data analysis of critical transitions in financial networks, in: Springer Proceedings in Complexity, Springer International Publishing, (ISSN: 2213-8692) ISBN: 9783319554716, 2017, pp. 47–59, http://dx.doi.org/10.1007/978-3-319-55471-6_5.
[25] M. Gidea, Y. Katz, Topological data analysis of financial time series: Landscapes of crashes, Phys. A (ISSN: 0378-4371) 491 (2018) 820–834, http://dx.doi.org/10.1016/j.physa.2017.09.028.
[26] M.S. Ismail, M.S.M. Noorani, M. Ismail, F.A. Razak, M.A. Alias, Early warning signals of financial crises using persistent homology, Phys. A (ISSN: 0378-4371) 586 (2022) 126459, http://dx.doi.org/10.1016/j.physa.2021.126459.
[27] W. Qiu, S. Rudkin, P. Dłotko, Refining understanding of corporate failure through a topological data analysis mapping of altman's Z-score model, Expert Syst. Appl. (ISSN: 0957-4174) 156 (2020) 113475, http://dx.doi.org/10.1016/j.eswa.2020.113475.
[28] E. Baitinger, S. Flegel, The better turbulence index? Forecasting adverse financial markets regimes with persistent homology, Financial Mark. Portfolio Manag. (ISSN: 2373-8529) 35 (3) (2021) 277–308, http://dx.doi.org/10.1007/s11408-020-00377-x.
[29] A. Goel, P. Pasricha, A. Mehra, Topological data analysis in investment decisions, Expert Syst. Appl. (ISSN: 0957-4174) 147 (2020) 113222, http://dx.doi.org/10.1016/j.eswa.2020.113222.
[30] H.G. Souto, Topological tail dependence: Evidence from forecasting realized volatility, J. Finance Data Sci. (ISSN: 2405-9188) 9 (2023) 100107, http://dx.doi.org/10.1016/j.jfds.2023.100107.
[31] H.G. Souto, Corrigendum to "topological tail dependence: Evidence from forecasting realized volatility" [the journal of finance and data science 9 (2023) 100107], J. Finance Data Sci. (ISSN: 2405-9188) (2024) 100135, http://dx.doi.org/10.1016/j.jfds.2024.100135.
[32] I. Fortin, C. Kuzmics, Tail-dependence in stock-return pairs, Intell. Syst. Account. Finance Manage. (ISSN: 1099-1174) 11 (2) (2002) 89–107, http://dx.doi.org/10.1002/isaf.216.
[33] F. Chesnay, E. Jondeau, Does correlation between stock returns really increase during turbulent periods? Econ. Notes (ISSN: 1468-0300) 30 (1) (2001) 53–80, http://dx.doi.org/10.1111/1468-0300.00047.
[34] Z. Gu, R. Ibragimov, The "cubic law of the stock returns" in emerging markets, J. Empir. Financ. (ISSN: 0927-5398) 46 (2018) 182–190, http://dx.doi.org/10.1016/j.jempfin.2017.11.008.
[35] R. Laudan, L. Laudan, A. Donovan, Testing theories of scientific change, in: Scrutinizing Science, Springer Netherlands, ISBN: 9789400928558, 1988, pp. 3–44, http://dx.doi.org/10.1007/978-94-009-2855-8_1.
[36] W.D. Berry, M. Golder, D. Milton, Improving tests of theories positing interaction, J. Polit. (ISSN: 1468-2508) 74 (3) (2012) 653–671, http://dx.doi.org/10.1017/s0022381612000199.
[37] M.S. Ulriksen, N. Dadalauri, Single case studies and theory-testing: the knots and dots of the process-tracing method, Int. J. Soc. Res. Methodol. (ISSN: 1464-5300) 19 (2) (2014) 223–239, http://dx.doi.org/10.1080/13645579.2014.979718.
[38] E. Sirakaya, A.G. Woodside, Building and testing theories of decision making by travellers, Tour. Manag. (ISSN: 0261-5177) 26 (6) (2005) 815–832, http://dx.doi.org/10.1016/j.tourman.2004.05.004.
[39] E. Cerin, A. Barnett, T. Baranowski, Testing theories of dietary behavior change in youth using the mediating variable model with intervention programs, J. Nutr. Educ. Behav. (ISSN: 1499-4046) 41 (5) (2009) 309–318, http://dx.doi.org/10.1016/j.jneb.2009.03.129.
[40] C. Press, D. Yon, C. Heyes, Building better theories, Curr. Biol. (ISSN: 0960-9822) 32 (1) (2022) R13–R17, http://dx.doi.org/10.1016/j.cub.2021.11.027.
[41] H. Edelsbrunner, J.L. Harer, ComputationalTopology: an Introduction, American Mathematical Society, 2022.
[42] B. Rieck, Topological data analysis for machine learning lecture, 2, 2020, URL https://bastian.rieck.me/talks/ECML_PKDD_2020_Lecture_2.pdf.
[43] M. Beine, A. Cosma, R. Vermeulen, The dark side of global integration: Increasing tail dependence, J. Bank. Financ. (ISSN: 0378-4266) 34 (1) (2010) 184–192, http://dx.doi.org/10.1016/j.jbankfin.2009.07.014.
[44] H. White, T.-H. Kim, S. Manganelli, VAR for VaR: Measuring tail dependence using multivariate regression quantiles, J. Econometrics (ISSN: 0304-4076) 187 (1) (2015) 169–188, http://dx.doi.org/10.1016/j.jeconom.2015.02.004.
[45] K. Jebran, S. Chen, I. Ullah, S.S. Mirza, Does volatility spillover among stock markets varies from normal to turbulent periods? Evidence from emerging markets of Asia, J. Finance Data Sci. (ISSN: 2405-9188) 3 (1–4) (2017) 20–30, http://dx.doi.org/10.1016/j.jfds.2017.06.001.
[46] C.M. Pereira, R.F. de Mello, Persistent homology for time series and spatial data clustering, Expert Syst. Appl. (ISSN: 0957-4174) 42 (15–16) (2015) 6026–6038, http://dx.doi.org/10.1016/j.eswa.2015.04.010.
[47] D. Shnier, M.A. Voineagu, I. Voineagu, Persistent homology analysis of brain transcriptome data in autism, J. R. Soc. Interface (ISSN: 1742-5662) 16 (158) (2019) 20190531, http://dx.doi.org/10.1098/rsif.2019.0531.
[48] L.Y. Liu, A.J. Patton, K. Sheppard, Does anything beat 5-minute RV? A comparison of realized measures across multiple asset classes, J. Econometrics (ISSN: 0304-4076) 187 (1) (2015) 293–311, http://dx.doi.org/10.1016/j.jeconom.2015.02.008.
[49] F. Corsi, A simple approximate long-memory model of realized volatility, J. Financ. Econom. (ISSN: 1479-8417) 7 (2) (2009) 174–196, http://dx.doi.org/10.1093/jjfinec/nbp001.
[50] M. Caporin, G.G. Velo, Realized range volatility forecasting: Dynamic features and predictive variables, Int. Rev. Econ. Finance (ISSN: 1059-0560) 40 (2015) 98–112, http://dx.doi.org/10.1016/j.iref.2015.02.021.
[51] H. Asgharian, C. Christiansen, A.J. Hou, The effect of uncertainty on stock market volatility and correlation, J. Bank. Financ. (ISSN: 0378-4266) 154 (2023) 106929, http://dx.doi.org/10.1016/j.jbankfin.2023.106929.
[52] A. Shojaie, E.B. Fox, Granger causality: A review and recent advances, Annu. Rev. Stat. Appl. (ISSN: 2326-831X) 9 (1) (2022) 289–319, http://dx.doi.org/10.1146/annurev-statistics-040120-010930.
[53] J.R. McCrorie, M.J. Chambers, Granger causality and the sampling of economic processes, J. Econometrics (ISSN: 0304-4076) 132 (2) (2006) 311–336, http://dx.doi.org/10.1016/j.jeconom.2005.02.002.
[54] H. White, D. Pettenuzzo, Granger causality, exogeneity, cointegration, and economic policy analysis, J. Econometrics (ISSN: 0304-4076) 178 (2014) 316–330, http://dx.doi.org/10.1016/j.jeconom.2013.08.030.
[55] L. Lopez, S. Weber, Testing for granger causality in panel data, Stata J.: Promot. Commun. Stat. Stata (ISSN: 1536-8734) 17 (4) (2017) 972–984, http://dx.doi.org/10.1177/1536867x1801700412.
[56] M. Eichler, V. Didelez, On granger causality and the effect of interventions in time series, Lifetime Data Anal. (ISSN: 1572-9249) 16 (1) (2009) 3–32, http://dx.doi.org/10.1007/s10985-009-9143-3.
[57] V. Troster, Testing for Granger-causality in quantiles, Econometric Rev. (ISSN: 1532-4168) 37 (8) (2016) 850–866, http://dx.doi.org/10.1080/07474938.2016.1172400.
[58] S. Weber, L. Lopez, Applied Econometric Analysis using Cross Section and Panel Data, Springer Nature Singapore, ISBN: 9789819949021, 2024, pp. 539–570, http://dx.doi.org/10.1007/978-981-99-4902-1_18.
[59] V. Pontines, D. Luvsannyam, G. Bayarmagnai, Money-output revisited: Time-varying granger causality evidence from forty-three countries, Open Econ. Rev. (ISSN: 1573-708X) (2024) http://dx.doi.org/10.1007/s11079-024-09764-7.
[60] C.W.J. Granger, Investigating causal relations by econometric models and cross-spectral methods, Econometrica (ISSN: 0012-9682) 37 (3) (1969) 424, http://dx.doi.org/10.2307/1912791.
[61] V.R. Joseph, Optimal ratio for data splitting, Stat. Anal. Data Min.: ASA Data Sci. J. (ISSN: 1932-1872) 15 (4) (2022) 531–538, http://dx.doi.org/10.1002/sam.11583.
[62] M.Z. Naser, A.H. Alavi, Error metrics and performance fitness indicators for artificial intelligence and machine learning in engineering and sciences, Archit. Struct. Constr. (ISSN: 2730-9894) (2021) http://dx.doi.org/10.1007/s44150-021-00015-8.
[63] C. Zhang, X. Pu, M. Cucuringu, X. Dong, Graph neural networks for forecasting realized volatility with nonlinear spillover effects, SSRN Electr. J. (ISSN: 1556-5068) (2023) http://dx.doi.org/10.2139/ssrn.4375165.
[64] K.G. Olivares, C. Challu, G. Marcjasz, R. Weron, A. Dubrawski, Neural basis expansion analysis with exogenous variables: Forecasting electricity prices with NBEATSx, Int. J. Forecast. (ISSN: 0169-2070) 39 (2) (2023) 884–900, http://dx.doi.org/10.1016/j.ijforecast.2022.03.001.
[65] X. Wang, C. Li, C. Yi, X. Xu, J. Wang, Y. Zhang, EcoForecast: An interpretable data-driven approach for short-term macroeconomic forecasting using N-BEATS neural network, Eng. Appl. Artif. Intell. (ISSN: 0952-1976) 114 (2022) 105072, http://dx.doi.org/10.1016/j.engappai.2022.105072.

[66] M. Han, Z. Su, X. Na, Predict water quality using an improved deep learning method based on spatiotemporal feature correlated: a case study of the Tanghe reservoir in China, Stoch. Environ. Res. Risk Assess. (ISSN: 1436-3259) 37 (7) (2023) 2563–2575, http://dx.doi.org/10.1007/s00477-023-02405-4.

[67] H.G. Souto, A. Moradi, Introducing NBEATSx to realized volatility forecasting, Expert Syst. Appl. (ISSN: 0957-4174) 242 (2024) 122802, http://dx.doi.org/10.1016/j.eswa.2023.122802.

[68] F.X. Diebold, R.S. Mariano, Comparing predictive accuracy, J. Bus. Econom. Statist. (ISSN: 0735-0015) 13 (3) (1995) 253, http://dx.doi.org/10.2307/1392185.

[69] D. Harvey, S. Leybourne, P. Newbold, Testing the equality of prediction mean squared errors, Int. J. Forecast. (ISSN: 0169-2070) 13 (2) (1997) 281–291, http://dx.doi.org/10.1016/s0169-2070(96)00719-4.

[70] S.M. Lundberg, S.-I. Lee, A unified approach to interpreting model predictions, in: I. Guyon, U.V. Luxburg, S. Bengio, H. Wallach, R. Fergus, S. Vishwanathan, R. Garnett (Eds.), Advances in Neural Information Processing Systems, Vol. 30, Curran Associates, Inc., 2017, URL https://proceedings.neurips.cc/paper_files/paper/2017/file/8a20a8621978632d76c43dfd28b67767-Paper.pdf.

[71] K.E. Mokhtari, B.P. Higdon, A. Başar, Interpreting Financial Time Series with SHAP Values, IBM Corp., Toronto, Ontario, Canada, 2019, pp. 166–172.

[72] Y. Meng, N. Yang, Z. Qian, G. Zhang, What makes an online review more helpful: An interpretation framework using XGBoost and SHAP values, J. Theor. Appl. Electr. Commer. Res. (ISSN: 0718-1876) 16 (3) (2020) 466–490, http://dx.doi.org/10.3390/jtaer16030029.

[73] W.E. Marcílio, D.M. Eler, From explanations to feature selection: assessing SHAP values as feature selection mechanism, in: 2020 33rd SIBGRAPI Conference on Graphics, Patterns and Images, SIBGRAPI, 2020, pp. 340–347.

[74] M.L. Baptista, K. Goebel, E.M. Henriques, Relation between prognostics predictor evaluation metrics and local interpretability SHAP values, Artificial Intelligence (ISSN: 0004-3702) 306 (2022) 103667, http://dx.doi.org/10.1016/j.artint.2022.103667.

[75] D. Wang, S. Thunéll, U. Lindberg, L. Jiang, J. Trygg, M. Tysklind, Towards better process management in wastewater treatment plants: Process analytics based on SHAP values for tree-based machine learning methods, J. Environ. Manag. (ISSN: 0301-4797) 301 (2022) 113941, http://dx.doi.org/10.1016/j.jenvman.2021.113941.

[76] K. Futagami, Y. Fukazawa, N. Kapoor, T. Kito, Pairwise acquisition prediction with SHAP value interpretation, J. Finance Data Sci. (ISSN: 2405-9188) 7 (2021) 22–44, http://dx.doi.org/10.1016/j.jfds.2021.02.001.

[77] A. Wojtuch, R. Jankowski, S. Podlewska, How can SHAP values help to shape metabolic stability of chemical compounds? J. Cheminform. (ISSN: 1758-2946) 13 (1) (2021) http://dx.doi.org/10.1186/s13321-021-00542-y.

[78] C. Cakiroglu, S. Demir, M. Hakan Ozdemir, B. Latif Aylak, G. Sariisik, L. Abualigah, Data-driven interpretable ensemble learning methods for the prediction of wind turbine power incorporating SHAP analysis, Expert Syst. Appl. (ISSN: 0957-4174) 237 (2024) 121464, http://dx.doi.org/10.1016/j.eswa.2023.121464.

[79] V. Vimbi, N. Shaffi, M. Mahmud, Interpreting artificial intelligence models: a systematic review on the application of LIME and SHAP in Alzheimer's disease detection, Brain Inform. (ISSN: 2198-4026) 11 (1) (2024) http://dx.doi.org/10.1186/s40708-024-00222-1.

[80] T. Chen, C. Guestrin, Xgboost: A scalable tree boosting system, in: Proceedings of the 22nd ACM SIGKDD International Conference on Knowledge Discovery and Data Mining, KDD '16, ACM, 2016, http://dx.doi.org/10.1145/2939672.2939785.